

Decreased Dopamine D4 Receptor Expression Increases Extracellular Glutamate and Alters Its Regulation in Mouse Striatum

Theresa Currier Thomas^{1,2,3}, David K Grandy^{4,5}, Greg A Gerhardt^{1,2,3,6,7} and Paul EA Glaser^{*,1,2,3,6,8}

¹Department of Anatomy & Neurobiology, University of Kentucky Chandler Medical Center, Lexington, KY, USA; ²Center for Microelectrode Technology, University of Kentucky Chandler Medical Center, Lexington, KY, USA; ³Morris K Udall Parkinson's Disease Research Center of Excellence, University of Kentucky Chandler Medical Center, Lexington, KY, USA; ⁴Department of Physiology, Oregon Health and Science University, Portland, OR, USA; ⁵Department of Pharmacology, Oregon Health and Science University, Portland, OR, USA; ⁶Department of Psychiatry, University of Kentucky Chandler Medical Center, Lexington, KY, USA; ⁷Department of Neurology, University of Kentucky Chandler Medical Center, Lexington, KY, USA; ⁸Department of Pediatrics, University of Kentucky Chandler Medical Center, Lexington, KY, USA

To better understand the effect of the dopamine D4 receptor (DRD4) on glutamate (Glu) neurotransmission in the brain, we utilized transgenic mice with partial or complete removal of functional DRD4 plasma membrane expression (DRD4+/- and DRD4-/-, respectively). We measured resting extracellular Glu levels, Glu clearance kinetics, and KCl-evoked release of Glu in the striatum and nucleus accumbens core of these mice using *in vivo* amperometry coupled to a novel microelectrode array configured for sub-second detection of Glu. Recordings from DRD4-/- and DRD4+/- mice were compared with their wild-type littermates (DRD4+/+). Resting extracellular levels of Glu were increased in the striatum of DRD4-/- mice ($p < 0.01$). Glu clearance kinetics were significantly decreased in the dorsal striatum of DRD4-/- mice ($p < 0.05$). KCl-evoked overflow of Glu was reliably measured but unchanged in the striatum of the three groups. By contrast, no changes in resting Glu, Glu uptake kinetics, or KCl-evoked release of Glu were observed in the nucleus accumbens core among the three genotypes. These data indicate that the DRD4 receptor is involved in modulation of Glu neurotransmission, primarily in the striatum. A better understanding of Glu control by the DRD4 may improve our understanding of the physiological role of the DRD4 in disorders such as attention-deficit/hyperactivity disorder and schizophrenia.

Neuropsychopharmacology (2009) **34**, 436–445; doi:10.1038/npp.2008.74; published online 4 June 2008

Keywords: dopamine D4 receptor; glutamate; striatum; nucleus accumbens; amperometry; attention-deficit/hyperactivity disorder (ADHD)

INTRODUCTION

The dopamine (DA) D4 receptor (DRD4) is part of the DA D2-like receptor subfamily (Jaber *et al*, 1996; Grady *et al*, 2003; Lichter *et al*, 1993; Cooper *et al*, 2003). On binding DA, this G-protein-coupled receptor undergoes a conformational change activating the inhibitory α -subunit that interacts with signaling mechanisms resulting in several downstream signaling events including (but not limited to) inhibition of adenylate cyclase, stimulation of arachidonic acid release, and modulation of G-protein-regulated inwardly rectifying potassium channels (Jaber *et al*, 1996; Tarazi *et al*, 2004; Oak *et al*, 2000). At a behavioral level, it has been shown that DRD4 plays a role in novelty seeking,

hyperactivity, and impaired behavioral inhibition in rodents, nonhuman primates, and humans (Ebstein *et al*, 1996; Avale *et al*, 2004; Zhang *et al*, 2001, 2002; Benjamin *et al*, 1996). Meta-analysis has indicated a higher frequency of a seven-repeat polymorphism in the D4 receptor in patients and relatives with attention-deficit/hyperactivity disorder (ADHD). Additionally, DRD4 alleles have been variously implicated in schizophrenia, perfectionism, migraine severity, and smoking (Bachner-Melman *et al*, 2007; de Sousa *et al*, 2007; Seeman *et al*, 1993; Guo and Tong, 2006).

The DRD4 is primarily expressed on pyramidal neurons and interneurons in the prefrontal cortex, but there is also support for DRD4 localization on medium spiny neurons in the basal ganglia (striatum, Str; and nucleus accumbens core, NAc), throughout the limbic system and in the thalamus of rodents (Mrzljak *et al*, 1996; Ariano *et al*, 1997a, 1997b; Tarazi *et al*, 2004; Gan *et al*, 2004; Cooper *et al*, 2003). In a study by Rivera *et al* (2002), DRD4s were found to be in higher concentrations in the densely packed neuron bundles, known as striosomes, of the Str in comparison with

*Correspondence: Dr PEA Glaser, Department of Psychiatry, University of Kentucky, 306 Whitney-Hendrickson Facility, 800 Rose Street, Lexington, KY 40536-0098, USA, Tel: +1 859 323 4531, Fax: +1 859 257 5310, E-mail: pglas0@uky.edu

Received 11 January 2008; revised 4 April 2008; accepted 16 April 2008

the more background neurons known as matrix. The striosomes receive input from limbic areas, cingulate cortex, and thalamus, indicating a role for DRD4 in regulation of the cortico-striatal-thalamic loop (Rivera *et al*, 2002). Three of the five proposed partially closed cortico-striatal-thalamic circuits are predicted to be associated with ADHD (Sagvolden *et al*, 2005; Alexander *et al*, 1986); therefore, it is possible to speculate that DRD4s may modulate part of this circuitry and lead to some of the behaviors in ADHD. Glutamate (Glu) is the main neurotransmitter for multiple connections in this circuit; therefore, understanding direct and indirect glutamatergic modulation in an *in vivo* setting will be essential in working out the pathophysiology of multiple brain disorders.

Until now, it has been difficult to study the neurochemical effects of DRD4s, because commercially available ligands for the DRD4 are nonspecific (Hai-Bin *et al*, 2005; Defagot *et al*, 2000). An alternative approach is to use wild-type (DRD4+/+), heterozygous (DRD4+/-), and knockout (DRD4-/-) mice for these studies (Rubinstein *et al*, 1997). Using biotinylation and western blotting, Rubinstein *et al* (1997) showed that there was no expression of the DRD4 in DRD4-/- mice and a 50% reduction of DRD4 expression in the DRD4+/- mice. Rubinstein *et al* (2001) presented evidence that the DRD4-/- mice exhibit cortical hyperexcitability using immunohistochemical, electrophysiological, pharmacological, and ultrastructural methods. Their results were consistent with the interpretation that DRD4 activation in DRD4+/+ mice has an inhibitory influence on Glu-containing pyramidal neurons in the frontal cortex (Rubinstein *et al*, 2001). With the lack of inhibitory modulation as a result of no functional DRD4s in the prefrontal cortex of DRD4-/- mice, we would expect decreased inhibition of glutamatergic pyramidal neuron firing. This would result in increased firing of Glu-containing neurons, and, thus, changes in Glu neurotransmission in the Str and NAc. At this time, no direct studies of resting extracellular Glu, Glu clearance, and evoked Glu release have been investigated in these animals.

In a recent study, we demonstrated that DRD4-/- mice have reduced levels of resting extracellular DA and decreased potassium (KCl)-evoked DA in the Str and NAc (Thomas *et al*, 2007). The purpose of the present studies was to further characterize the DRD4-/- mice with respect to Glu neurotransmission in these areas. First, we characterized resting extracellular levels of Glu in the Str and NAc of DRD4+/+, DRD4+/-, and DRD4-/- mice. Second, we characterized Glu clearance by local application of exogenous Glu in the three animal groups. Third, we characterized KCl-evoked Glu in the Str and NAc of these animals. We hypothesized that DRD4 mice would show evidence of a hyperglutamatergic state.

MATERIALS AND METHODS

Animals

Male mice (5–7 months) descended from the original F₂ hybrid of mice with a truncated and non-expressing DRD4 gene (DRD4-/-) (129/SvEv × C57BL/6J; Rubinstein *et al*, 1997) were derived by backcrossing the heterozygous (DRD4+/-) mouse line for 20 generations (N20). In all experiments, the DRD4-/- mice (*n* = 7–9) and DRD4+/-

(*n* = 6–8) were compared with litter-matched DRD4+/+ (*n* = 7–9) animals. Mice were group-housed (2–4 per cage) with unlimited access to food and water. Mice were maintained on a 12-h light/dark cycle (lights on at 0600 hours). Protocols for animal use were approved by the Institutional Animal Care and Use Committee, which is Association for Assessment and Accreditation of Laboratory Animal Care International approved. All procedures were carried out in accordance with the National Institutes of Health Guide for Care and Use of Laboratory Animals.

Microelectrode Array Preparation and *In Vitro* Calibrations

Microelectrode preparation for Glu recordings. Ceramic-based microelectrode arrays (MEAs) that contained four platinum (Pt) recording surfaces were prepared to selectively measure Glu (Figure 1a). These electrodes were fabricated for *in vivo* recordings using published methods (Burmeister *et al*, 2000, 2002; Nickell *et al*, 2005). All four sites were electroplated with meta-phenylenediamine (mPD) by applying a potential of +0.5 V to the Pt sites *vs* a silver/silver chloride (Ag/AgCl) reference electrode (Bioanalytical Systems, RE-5) in a deoxygenated 0.05 M phosphate-buffered saline (PBS, pH 7.1–7.4) with 5.0 mM mPD. The mPD forms a size-exclusion layer over the sites, blocking DA, ascorbic acid (AA), DOPAC, and other electroactive compounds. Pt sites 1 and 2 (see Figure 1a) were then coated with glutamate oxidase (Glu-Ox) within an inert protein matrix of bovine serum albumin (BSA) and glutaraldehyde (Glut), enabling these sites to detect Glu levels on a sub-second timescale with low levels of detection (~0.2 μM). Sites 3 and 4 were coated with only BSA and Glut (Burmeister and Gerhardt, 2001; Day *et al*, 2006). In the presence of Glu-Ox, Glu was broken down into α-ketoglutarate and peroxide (H₂O₂). The H₂O₂ is small enough to traverse the mPD layer and was readily oxidized and recorded as current using FAST-16 equipment (Fast Analytical Sensor Technology (FAST); Quanten LLC, Nicholasville, KY).

Microelectrode calibration. The microelectrode was submerged in 40 ml of 0.05 M PBS (pH 7.1–7.4) warmed to 37°C using a circulating water bath (Gaymar Industries Inc., Orchard Park, NY), and stirred using a magnetic stir bar and battery operated stir plate (Barnart Co.). Measurements were made using an applied potential of +0.7 V *vs* an Ag/AgCl reference electrode (Bioanalytical Systems; RE-5). Signals were amplified by the headstage gain (2 nA/V) and a secondary gain of 10 times for a final gain of 200 pA/V. Following a 10- to 20-min equilibration, aliquots of stock solutions were added to the PBS (see Figure 1b). The final concentrations of the stock solutions in the 40-ml PBS were 250 μM AA; 20, 40, and 60 μM L-glutamate (L-Glu); 2 and 4 μM DA; and 8.8 μM H₂O₂. AA and DA were used to ensure that the mPD coating was blocking these electroactive molecules that are abundant within the Str and NAc. From the calibration, the slope (electrodes sensitivity to L-Glu), selectivity (capabilities of recording L-Glu over AA), and limit of detection (LOD—smallest amount of detectable Glu) were calculated: average values for slope were -7.5 ± 5.0 pA/μM, for selectivity were 214 ± 48 to 1, and for LOD were 0.72 ± 0.12 μM (*n* = 28 electrodes; 56 Glu recording sites).

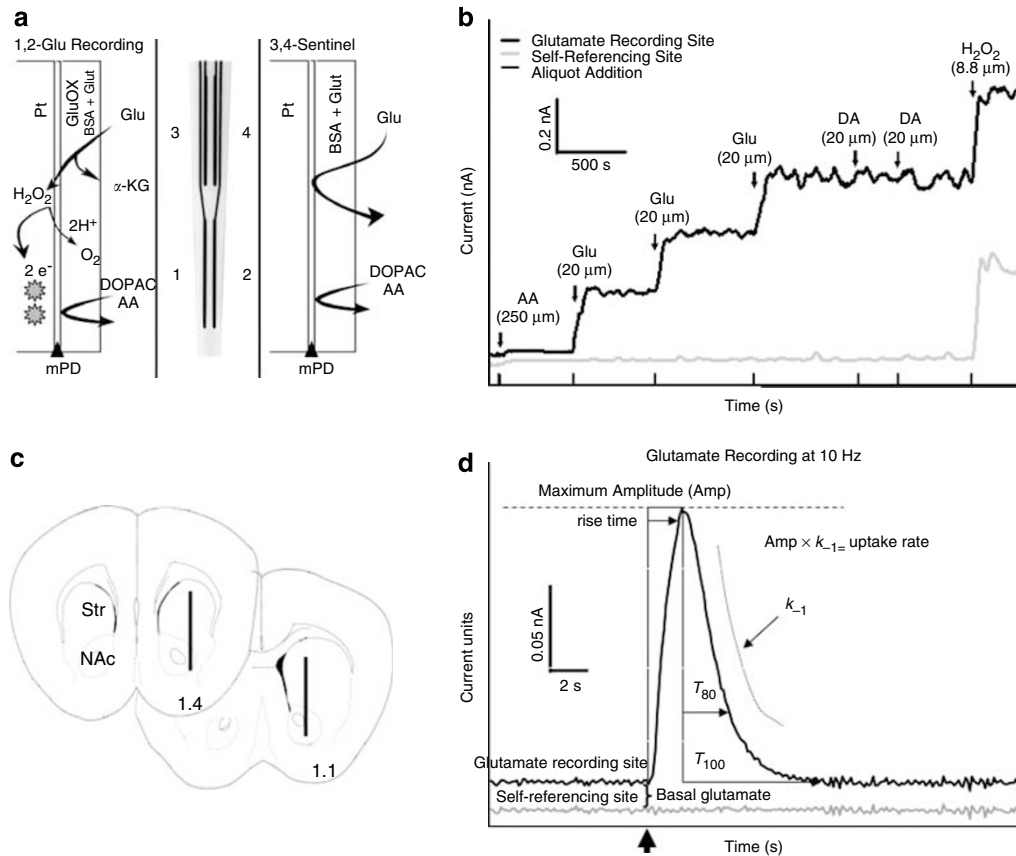


Figure 1 (a) Schematic diagram of multisite enzyme-based MEA showing the coating layers and configuration of Pt recording sites. These MEAs are designed for self-referencing recordings that provide real-time measures of Glu clearance and resting extracellular Glu levels. Sites 1 and 2 are prepared to measure Glu by coating with a mixture of Glu-ox, BSA, and Glut. Sites 3 and 4 serve as self-referencing sites and are coated with only BSA and Glut. An electroplated layer of mPD forms a size-exclusion layer minimizing electroactive molecules (AA, DA) from interacting with the electrode sites. The size of the electrode sites is $15 \times 333 \mu\text{m}$. The distance between the pairs of electrodes (1/2 vs 3/4) is $100 \mu\text{m}$. The distance between sites 1 and 2 is $30 \mu\text{m}$. (b) A representative recording from *in vitro* MEA calibration. Only one Glu recording site and one self-referencing site are represented. The vertical bars on the x-axis represent the addition of each analyte (AA, Glu, DA, and H_2O_2). AA has little effect on the baseline on the MEA sites. Three sequential additions of 20 mM Glu ($40 \mu\text{l}$ each) resulted in stepwise increases in current recorded for site 1. Two aliquots of DA are added to ensure mPD integrity (as DA is easily oxidized on a Pt surface at an applied potential of 0.7 V). A final aliquot of peroxide (H_2O_2) is used to ensure that all channels are working. (c) MEA placement within the mouse Str and NAc. The diagram shows the approximate location of the Glu recording sites within the Str and NAc at locations 1.1 and 1.4 mm from bregma (modified from Franklin and Paxinos, 1997). The MEA was moved in $350 \mu\text{m}$ increments throughout the dorsomedial Str and NAc. (d) Representative Glu clearance recording in mouse Str. A recording of Glu clearance in the Str of a DRD4 $+/+$ mouse. The large arrow on the x-axis indicates the time point of local application of exogenous Glu. The time from local application to maximum amplitude of the signal is referred to as rise time. Once the maximum amplitude is reached, three separate measurements are acquired as Glu is cleared from the extracellular space: the uptake rate constant (k_{-1}), the uptake rate, and the T_{80} . The T_{80} is the time point at which 80% of the Glu is cleared in reference to the maximum amplitude (Cass *et al*, 1993; Cass and Gerhardt, 1995).

Micropipette attachment. After the MEA was calibrated, a single barrel glass capillary with filament ($1.0 \times 0.58 \text{ mm}^2$, $6''$; A-M Systems Inc., Everett, WA) was pulled using a Kopf pipette puller (David Kopf Instruments, Tujunga, CA) and bumped for an inner diameter of $10\text{--}12 \mu\text{m}$. The tip of the micropipette was placed between the four recording sites, approximately $50\text{--}80 \mu\text{m}$ away from the electrode surface and secured using Sticky Wax (Kerr Manufacturing Co., Detroit, MI). For these studies, the average distance was approximately $65 \mu\text{m}$.

Surgeries for Amperometric Recordings

Mice were anesthetized using intraperitoneal injections of 10% urethane solution (1.25 g/kg) and placed in a stereotaxic frame (David Kopf Instruments) fitted with a

CunninghamTM Mouse and Neonatal Rat Adaptor (Stoelting Co., Wood Dale, IL). A circulating heating pad (Gaymar Industries Inc.) coupled to a rectal temperature probe (Yellow Spring Instrument Co., Yellow Springs, OH) was used to maintain body temperature at 37°C . The skull overlying the medial cortex was removed bilaterally. An additional hole, remote from the surgery site, was opened for an Ag/AgCl reference electrode (Hascup *et al*, 2006).

In Vivo Experimental Protocol

Prior to placement of the MEA micropipette assembly, the micropipette was filled with isotonic $125 \mu\text{M}$ Glu ($125 \mu\text{M}$ L-Glu in 9% physiological saline; pH 7.2–7.4) or 35 mM KCl solution (35 mM KCl, 114 mM NaCl, 2.5 mM CaCl_2 ; pH 7.2–7.4) using a combination of a 1-ml syringe filled with

Glu or KCl solutions, a 0.22- μm sterile syringe filter (Costar Corporation), and a 4" pulled needle (30 gauge, beveled tip; Popper and Son Inc., NY). The MEA micropipette assembly was positioned in the brain according to the following stereotaxic coordinates where all anterior–posterior (AP) measures were from bregma, medial–lateral (ML) measures were from midline, and dorsal–ventral (DV) measures were from dura: AP: +1.1 mm, ML: \pm 1.1 mm, DV: -2.25 – 4.1 mm; and AP: +1.4 mm, ML: \pm 1.4 mm, DV: -2.25 – 4.1 mm according to the Mouse Brain in Stereotaxic Coordinates (see Figure 1d; Franklin and Paxinos, 1997). A potential of +0.7 V was applied vs a miniature Ag/AgCl reference electrode, and the data were displayed at a frequency of 2 Hz. Recordings made at depths of 2.15, 2.5, and 2.85 mm were used for measures in the dorsomedial Str and recordings at 3.65 and 4.0 mm were used for measures in the NAc (see Figure 1c).

Nanoliter volumes of Glu or KCl were locally applied to tissue by pressure ejection using a Picospritzer II connected to the open end of the micropipette by plastic tubing (Parker Hannifin Corp., General Valve Corporation). Pressure was applied at 5–25 p.s.i. for 1 s in all of the experiments. The volume of Glu or KCl delivered was measured by determining the amount of fluid ejected from the micropipette using a dissection microscope fitted with a calibrated reticule (Cass *et al*, 1992; Friedemann and Gerhardt, 1992).

Measurements of resting levels and Glu clearance parameters. Upon stereotaxic placement of the MEA micropipette assembly (AP: +1.1 mm, ML: \pm 1.1 mm, DV: -2.15 – 4.0 mm), 10–20 min of baseline data were acquired. Resting levels of Glu were measured by averaging 30 s of baseline recordings prior to application of Glu or KCl. Then, 125 μM Glu solution was locally applied every 30–60 s for a total of 10 recordings. The MEA was then lowered in 350 μm increments. Baseline recordings were acquired for 5–10 min and the recordings were repeated. Parameters from 3 of the 10 signals ranging from 10–30 μM in amplitude were averaged for each Pt electrode site at each depth. The calculations from the left and right hemispheres were averaged for a single measurement per depth in all mice. Signals were analyzed for time required to rise to maximum amplitude (rise time), time for 80% of the signal to decay from maximum amplitude (T_{80}), and the rate of uptake (see Figure 1d). The uptake rate was calculated by multiplying the rate constant (referred to as k_{-1} ; units = per seconds) by the maximum amplitude (uptake rate = $\mu\text{M/s}$; Hascup *et al*, 2006). All data from local applications of Glu were pooled into a single data set. Amplitude-matched signals were compared with assess genotypic differences in the rates of clearance of exogenous Glu. Volume-matched signals were compared to determine capacity to clear similar amounts of exogenous Glu (Hebert and Gerhardt, 1999).

KCl-induced release of Glu. KCl was locally applied by pressure ejection into the Str and NAc (AP: +1.4 mm, ML: \pm 1.4 mm, DV: -2.0 – 4.1 mm) (Franklin and Paxinos, 1997), once a steady-state signal was achieved, the effects of a single local application of KCl solution on Glu release were determined (Gerhardt *et al*, 1985, 1986, 1987; Gerhardt and Palmer, 1987; Luthman *et al*, 1993; Cass *et al*, 1993). Data

regarding amperometric recordings were volume matched (12.5–100 nl) prior to data analysis. Recordings from sites 1 and 2 were averaged, and data from both hemispheres were averaged to one data point per depth.

Materials

Urethane, L-Glu, DA, AA, sodium chloride, potassium chloride, calcium chloride, and 1,3-phenylenediamine dihydrochloride were obtained from Sigma (St Louis, MO). MEAs were provided by Quanteon LLC and constructed in conjunction with Thin Films Technology Inc. (Buellton, CA).

Histology

Brains were removed and processed for histological evaluation of microelectrode recording tracts. Only data from histologically confirmed placements of microelectrodes within the Str and NAc were used for final data analysis.

Data Analysis

Data from the side-by-side recordings were averaged and used as a single data point. If only one electrode site provided usable data, then the recordings were reported as from that site. No outliers were removed from the presented data, but some data were excluded due to volume or amplitude-matching criterion. To determine statistical significance ($p < 0.05$) processed data were analyzed using a one-way ANOVA with Tukey's *post hoc* comparison across all genotypes (Graphpad Prism 4.0).

RESULTS

Resting Levels of Extracellular Glu in the Str and NAc

To evaluate the effect of DRD4 expression level on resting levels of Glu, we compared extracellular Glu levels across genotypes in the Str and NAc (see Figure 2). Resting levels of Glu were seen to be increased by 64% in the Str of DRD4 $-/-$ mice in comparison with their wild-type littermates (DRD4 $+/+$: $1.5 \pm 0.3 \mu\text{M}$, $n = 7$; signals = 45; DRD4 $-/-$: $2.4 \pm 0.2 \mu\text{M}$, $n = 9$, signals = 45; $p < 0.01$; see Figure 2). There were no significant changes in the NAc, although there was a trend for slightly higher Glu levels in the DRD4 $-/-$ mice (DRD4 $+/+$: $1.3 \pm 0.2 \mu\text{M}$; DRD4 $-/-$: $1.8 \pm 0.2 \mu\text{M}$; $p < 0.10$). The DRD4 $+/-$ mice were most similar to the DRD4 $+/+$ mice in both the Str and NAc (Str: $1.4 \pm 0.2 \mu\text{M}$, $n = 7$; signals = 35; NAc: $1.2 \pm 0.2 \mu\text{M}$, $n = 6$; signals = 22). These data indicate that the loss of DRD4 expression resulted in increased resting Glu levels in the Str.

Glu Clearance in the Str and NAc

The *in vivo* activity of Glu uptake was examined with a high degree of temporal and spatial resolution by locally applying exogenous Glu to the tissue and measuring the presence and successive clearance kinetics of the signals (Cass *et al*, 1993). Resulting data provided kinetic measures that allowed us to evaluate removal of exogenous Glu from the extracellular space within the Str and NAc. Statistical

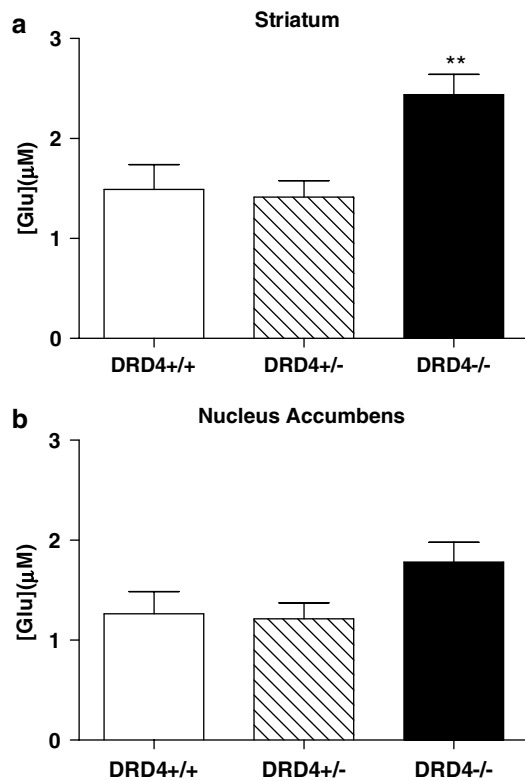


Figure 2 Resting extracellular Glu levels in the Str and NAc. (a) This bar graph demonstrates the differences in extracellular levels of Glu in the Str of DRD4+/+, DRD4+/-, and DRD4-/- (** $p < 0.01$). (b) Extracellular levels of Glu in the NAc did not significantly differ from each other. Values represent the mean \pm SEM.

comparisons were made on amplitude-matched data to make sure that variations in maximum amplitude would not contribute to changes in rise time, uptake rate, and T_{80} . In the Str, average amplitudes were $20.0 \pm 0.8 \mu\text{M}$ ($n = 8$; signals = 24), $19.5 \pm 1.2 \mu\text{M}$ ($n = 8$; signals = 23), and $18.9 \pm 1.0 \mu\text{M}$ ($n = 9$; signals = 26) in the DRD4+/+, DRD4+/-, and DRD4-/- mice, respectively. The locally applied Glu signals took approximately 1–2 s to rise to maximum amplitude (rise time). Rise time did not vary significantly between genotypes in the Str or the NAc. Uptake rate in the Str was significantly slower in the DRD4-/- mice in comparison with DRD4+/+ mice (5.3 ± 0.5 vs $7.4 \pm 0.6 \mu\text{M/s}$; $p < 0.05$; see Figure 3a and c). The slower uptake rate of Glu from the extracellular space is supported by a trend of increased time taken for 80% of the Glu to decay from the recording site (T_{80} ; DRD4+/+: 3.2 ± 0.2 s vs DRD4-/-: 4.4 ± 0.5 s; Figure 3). Kinetic measures of Glu clearance in the NAc showed no significant differences among genotypes (Figure 3b). Thus, we concluded that only the uptake rate was decreased in the Str of the DRD4-/- mice.

To investigate genotype-related changes in the Str and the capacity of NAc to clear exogenous Glu (Cass and Gerhardt, 1995), similar amounts of exogenous Glu were locally applied to the different genotypes, and the resulting maximum amplitudes and amplitudes per nanoliter were compared. Signal amplitude and normalized amplitude per nanoliter measures within the Str and NAc of DRD4+/+,

DRD4+/-, and DRD4-/- mice are presented in Table 1. There were no significant differences between genotypes in the Str or NAc, although a trend for higher levels of Glu per nanoliter were seen in the DRD4+/+ mice in both brain regions. Thus, there is likely similar surface expression of Glu transporters in the different genotypes.

KCl-Evoked Glu Release in the Str and NAc

To evaluate the effect of the DRD4 on synaptic release of Glu and to assess biologically relevant levels of evoked Glu release, we locally applied similar amounts of KCl to the Str and NAc of DRD4+/+, DRD4+/-, and DRD4-/- mice. Figure 4 depicts representative traces of KCl-evoked Glu signals in the three genotypes of mice from the Str. There were no significant differences in the amount of KCl-evoked Glu release, although there was a trend for higher amounts of KCl-evoked Glu overflow in the Str and NAc of the DRD4+/+ mice (see Table 2). The temporal properties of the signals were also not significantly different between the three groups of mice in the Str and NAc. Interestingly, the rise times for KCl-evoked Glu in the Str averaged 1.6 ± 0.1 s for the DRD4-/- mice, 1.4 ± 0.1 s for the DRD4+/- mice, and 1.2 ± 0.1 s for the DRD4+/+ mice. We also measured T_{80} in the three genotypes and found that these averaged 3.7 ± 0.2 s for the DRD4-/- mice, 3.6 ± 0.3 s for the DRD4+/- mice, and 3.4 ± 0.4 s for the DRD4+/+ mice in the Str. Similar rise times and T_{80} values were seen in the NAc (data not shown). Thus, although KCl produced robust changes in extracellular Glu, no significant differences were observed in the Str and NAc due to alterations in D4 expression.

DISCUSSION

We sought to understand the DRD4s involvement in Glu regulation in the Str and NAc of DRD4+/+, DRD4+/-, and DRD4-/- mice. *In vivo* amperometric studies showed a 64% increase in resting Glu levels in the Str of DRD4-/- mice. In addition, Glu clearance was significantly slower in the Str of DRD4-/- mice. Interestingly, these changes were not seen in the NAc. No statistically significant differences were observed in volume-matched Glu clearance studies or KCl-evoked Glu release in Str and NAc. No significant alterations were measured in the heterozygous mice indicating that greater than 50% loss of DRD4s is needed to measure the effects on Glu neurotransmission. Taken together, these data indicate a possible role for the DRD4 in the regulation of Glu in striatal circuitry.

Analyses of resting extracellular Glu levels in the past were often done by various forms of microdialysis (Espey *et al*, 1998; Behrens *et al*, 2002). This is the first study we know of looking at resting Glu levels in the Str and NAc of anesthetized C57BL/6J mice using a microelectrode technology. Espey *et al* (1998) reported levels at $0.9 \pm 0.1 \mu\text{M}$ in anesthetized C57BL/6J background mice using microdialysis. Behrens *et al* (2002) reported baseline levels of $0.7 \pm 0.1 \mu\text{M}$ in the Str of freely moving mice using microdialysis. Our microelectrode data showed striatal extracellular Glu levels of $1.5 \pm 0.2 \mu\text{M}$, almost twice that of the microdialysis studies. Variations in the resting

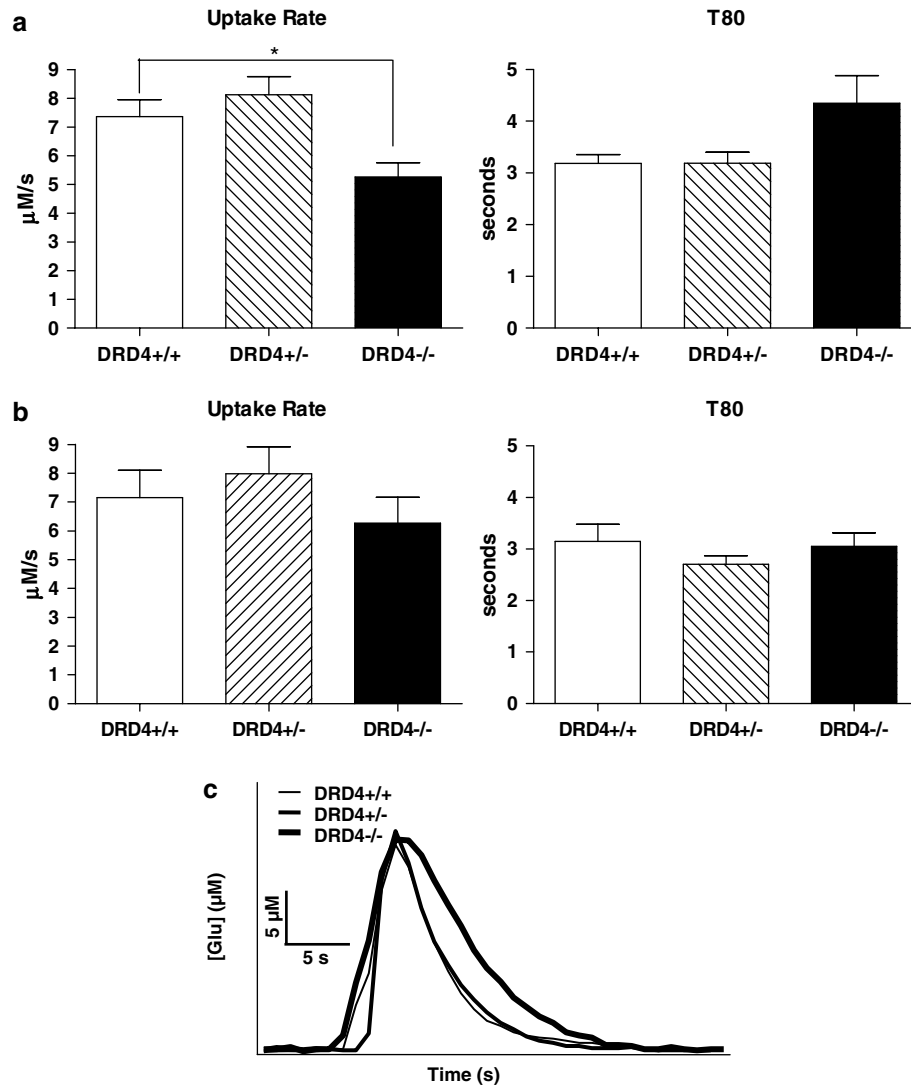


Figure 3 Glu clearance in the Str and NAc. (a) The bar graphs demonstrate changes in Glu clearance in the Str as a function of DRD4 expression. Uptake rate is significantly slower in the DRD4^{-/-} mice in comparison with their DRD4^{+/+} littermates (**p* < 0.05), and there was a trend for the *T*₈₀ values to be longer in DRD4^{-/-} mice. (b) The bar graphs show no significant changes in Glu clearance parameters in the NAc. Values represent the mean ± SEM. (c) Amplitude-matched recordings resulting from local application of Glu demonstrate differences seen in Glu clearance parameters from DRD4^{+/+}, DRD4^{+/-}, and DRD4^{-/-} mice in the Str.

Table I Capacity of Tissue to Clear Exogenous Glu

	Genotype	Volume (nl)	Amplitude (µM)	Amplitude per nanoliter (µM/nl)
Striatum	DRD4 ^{+/+} (<i>n</i> = 8)	42.7 ± 3.6	21.5 ± 1.4	0.72 ± 0.08
	DRD4 ^{+/-} (<i>n</i> = 8)	45.4 ± 4.3	18.5 ± 1.6	0.55 ± 0.09
	DRD4 ^{-/-} (<i>n</i> = 9)	43.1 ± 4.8	17.4 ± 1.4	0.59 ± 0.09
Nucleus accumbens	DRD4 ^{+/+} (<i>n</i> = 8)	41.0 ± 5.7	18.0 ± 1.2	0.95 ± 0.23
	DRD4 ^{+/-} (<i>n</i> = 8)	41.5 ± 5.9	17.5 ± 1.8	0.72 ± 0.18
	DRD4 ^{-/-} (<i>n</i> = 9)	40.5 ± 5.7	17.3 ± 1.6	0.73 ± 0.19

Similar volumes of exogenous Glu resulted in similar amplitudes and amplitudes per nanoliter measures in the Str and NAc (mean ± SEM).

Glu levels as recorded by *in vivo* amperometry and microdialysis may be multifactorial, including the different sizes of the probes and the temporal resolution of the

measures. The MEA is much smaller than the microdialysis probe, producing less cellular damage and likely recording much closer to intact synapses (Rutherford *et al*, 2007). In

anesthetized animal studies, microdialysis shows evidence of tissue disruption of at least 220–250 μm away from the probe (Borland *et al*, 2005), whereas the MEA showed evidence of some neuroinflammation only 50–100 μm away in a chronic study following 8 weeks *in vivo* (Rutherford *et al*, 2007). The temporal resolution of our MEA is an order of magnitude faster than the most sophisticated microdialysis techniques designed for measurement of amino acid neurotransmitters (Kennedy *et al*, 2002).

The microelectrode technology also has the advantage of being able to measure Glu clearance kinetics. Different uptake rates across genotypes indicate significant DRD4-related alterations in the duration of Glu in the extracellular space, which likely denotes the importance of the DRD4 in regulating Glu clearance. Glu was cleared approximately 29% slower in the Str of DRD4 $^{-/-}$ mice as compared with DRD4 $^{+/+}$ animals. It is not known whether the measured effects on uptake rate were a direct or indirect effect of DRD4 signaling loss. Although it is unlikely that a resting Glu concentration of 2.4 μM is saturating uptake sites, it is possible that the increased extracellular Glu levels interact with glial Glu receptors to affect Glu transport. Within the NAc, the uptake rate did not change as a function of the presence of the DRD4. Volume-matched clearance of exogenous Glu data also showed no significant changes in maximum amplitude. Another possible consequence of a slower Glu uptake rate could be that Glu remains in the extracellular space longer, resulting in altered postsynaptic signaling in the DRD4 $^{-/-}$ mice.

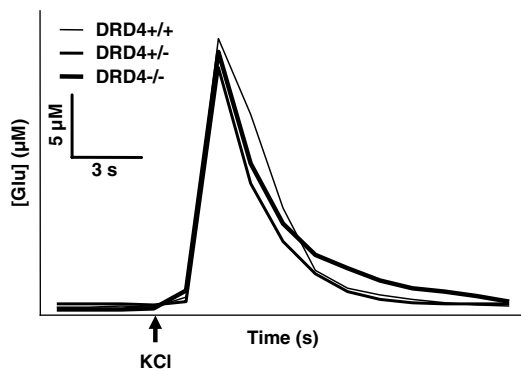


Figure 4 KCl-evoked Glu release in the mouse Str. Recordings of Glu signals evoked by locally applied KCl solution are shown. These signals were similar in amplitude and clearance time in both the Str and NAc.

Another parameter of the Glu clearance system is B_{max} , or the surface expression of Glu transporters located on glia and neurons. Previous research in our lab found that changes in clearance parameters were correlated with changes in the surface expression of Glu transporters (Nickell *et al*, 2007). Previous studies for DA in the Str, and NAc of F344 rats demonstrated that signal amplitudes of the applied neurotransmitter normalized for the amount applied, was correlated with B_{max} -values for DA transporters (as assessed by radioligand binding and uptake studies; Hebert and Gerhardt, 1999). Our correlation of relative *in vivo* B_{max} -values (amplitude per nanoliter of applied Glu, see Table 1) did not demonstrate significant differences between DRD4 $^{+/+}$, DRD4 $^{+/-}$, and DRD4 $^{-/-}$ mice. However, additional direct studies of the surface expression of Glu transporters on glia and neurons, and kinetic studies in the different animal groups are needed.

The mechanism by which resting levels of Glu are significantly increased in this study as a result of altered DRD4 expression is unknown, but several possibilities exist. The DRD4 has been localized to the axonal projections of glutamatergic corticostriatal neurons in the Str, where it can regulate the release of Glu (Berger *et al*, 2001). It was shown by Maura *et al* (1988) that activation of presynaptic DA D2-like receptors inhibits Glu release in striatal synaptosomes from rats. We have reported in previous work that extracellular DA is significantly decreased in the Str/NAc of DRD4 $^{-/-}$ mice (Thomas *et al*, 2007). Therefore, decreased activation of D2-like family receptors could lead to the resultant increase in resting Glu release. Corticostriatal projections can also provide a mechanism for increased resting Glu levels in the Str. The D4 receptor is also known to be postsynaptic in the prefrontal cortex and can influence resting Glu levels in the Str by inhibiting cell firing of the pyramidal neurons and the tonic function of the terminating synapses in the Str and NAc. When removing the D4 receptor, the inhibition is removed and these neurons fire more spontaneously (Rubinstein *et al*, 2001). This could account for the increase in tonic firing, which can also contribute to the increased resting levels of Glu seen in the Str. Contributions from DRD4 deletion on MSNs can potentially affect retrograde messengers (Thomas *et al*, 2007) as well as contribute to possible dysfunction in the striatopallidal pathway, which may facilitate a feed-forward effect of DRD4 loss within the

Table 2 KCl-Evoked Glu Release Data

	Genotype	Volume (nl)	Amplitude (μM)	Amplitude per nanoliter ($\mu\text{M}/\text{nl}$)
Striatum	DRD4 $^{+/+}$ ($n = 6$)	39.6 \pm 5.3	22.7 \pm 5.8	0.78 \pm 0.21
	DRD4 $^{+/-}$ ($n = 6$)	41.8 \pm 8.5	12.9 \pm 1.9	0.61 \pm 0.17
	DRD4 $^{-/-}$ ($n = 9$)	41.6 \pm 4.7	14.5 \pm 3.3	0.52 \pm 0.11
Nucleus accumbens	DRD4 $^{+/+}$ ($n = 6$)	40.7 \pm 6.5	15.8 \pm 5.2	0.88 \pm 0.46
	DRD4 $^{+/-}$ ($n = 6$)	39.6 \pm 5.0	7.5 \pm 1.0	0.23 \pm 0.03
	DRD4 $^{-/-}$ ($n = 8$)	41.0 \pm 4.6	9.9 \pm 2.3	0.34 \pm 0.11

Similar volumes of 35 mM KCl applied to the Str and NAc resulted in robust Glu release but no significant differences due to genotype were observed (mean \pm SEM).

cortico-striatal-thalamic circuit. The relative contributions of metabolic and neuronal pools of Glu to resting levels of Glu and the role of D4 receptors in astrocytic regulation of Glu still requires investigation.

One discrepancy we did not expect in these data was changes in the Str and not in the NAc. We know this is not due to changes in the MEA over time, because previous experiments have shown that Glu-selective sites maintain comparable sensitivity to Glu up to 7 days post implantation within the brain parenchyma (Rutherford *et al*, 2007). The organization of the corticostriatal projections are such that glutamatergic pyramidal neurons that have cell bodies mostly in lamina 5 (with some in 3 and 6) of the frontal cortex project to the Str and NAc (McGeorge and Faull, 1989). The DRD4 have a cellular distribution to these pyramidal neurons in lamina 5 (and some in 3) (Noain *et al*, 2006; Mrzljak *et al*, 1996; Ariano *et al*, 1997b); although Berger *et al* (2001) reported DRD4 localization mainly to layers 2–4 with only small amounts in 5. Our Glu and KCl data were taken from the dorsomedial Str, which has projections from the visual, cingulate, agranular insular cortex, motor 2 regions, and auditory parts of the cerebral cortex (McGeorge and Faull, 1989). The NAc has projections from similar areas, such as infralimbic and cingulate areas, but there is an increasing amount of projections from the hippocampus, entorhinal cortex, piriform cortex, amygdala, and subiculum (McGeorge and Faull, 1989). There is indication that these areas projecting to the NAc may have lower amounts of DRD4 influence (as compared with striatal projections) and, therefore, may not be as affected by loss of the DRD4, which may explain why we see data trends (Noain *et al*, 2006). Also, Rivera *et al* (2002) reported higher local expression of DRD4 in the Str in comparison with the NAc of rats, but the presence of DRD4 in these areas is debated (Noain *et al*, 2006). Our recordings were made in the NAc core. Changes in Glu due to DRD4 alterations are possible in the nucleus accumbens shell, but this area was not measured and needs to be studied.

One caveat of transgenic mice is that compensatory effects may be contributing to the neurochemical effects that we measured. The DRD4^{-/-} mice have been found to have increased expression of DA D1 receptors (DRD1) (+42%) and NMDA receptors (+40%) within the Str. Likewise, increased DRD1 (+39%) and NMDA (+31%) receptors in the NAc were also seen in DRD4^{-/-} mice in comparison to DRD4^{+/+} mice. NMDA receptors in the hippocampal CA1 and CA3 regions were also increased (21 and 25%). There were no changes in the amounts of DA D2 receptors (DRD2), AMPA, or kainate receptors between genotypes (Gan *et al*, 2004). Another study showed that DRD4^{-/-} mice expressed a nine-fold increase of DRD2s in the high-affinity state in comparison with DRD2s in the low-affinity state, whereas the DRD2 protein levels remained similar in both genotypes (Seeman *et al*, 2005). It has been shown that high-affinity DRD2s tend to be autoreceptors (Cooper *et al*, 2003). The compensatory effects on Glu neurotransmission resulting from increased levels of D1, NMDA, and D2 high-affinity receptors could be contributing to the findings reported in this paper and need to be investigated. Regardless, the compensatory effects pinpoint the importance of the DRD4 signaling in the Str

and strengthen the importance of DA and Glu interactions in these areas.

There is an increasing amount of research supporting a role for the Str in ADHD neurobiology (Durstun *et al*, 2003; Lou *et al*, 1989; Teicher *et al*, 2000). Furthermore, there is a growing interest in the role of Glu, whether it is through DA/Glu interactions or dysregulation of Glu neurotransmission, as a potential contributor to ADHD symptomatology (Carrey *et al*, 2003, 2007; MacMaster *et al*, 2003; Russell *et al*, 2005). Additionally, Carrey *et al* (2007) found evidence of increased levels of Glu in the Str of ADHD patients by c13 magnetic resonance imaging (MRI), which complemented the proton magnetic resonance spectroscopy studies done in 2003 (MacMaster *et al*, 2003). There is also evidence of striatal dysfunction in ADHD patients shown by emission topography and functional MRI studies (Lou *et al*, 1989; Teicher *et al*, 2000).

Various lines of research have correlated the DRD4 with behaviors and drug mechanisms, but the underlying neurochemistry of the DRD4 is not well understood. Using transgenic mice, we have demonstrated that alterations in DRD4 expression can alter multiple neurotransmitter systems, in this case, Glu. These studies support the role of DRD4 in presynaptic Glu regulation and suggest that alterations in DRD4 may lead to alterations in Glu function. Further studies will be needed to address the mechanisms involved.

ACKNOWLEDGEMENTS

These studies were supported by USPHS Grants DA07262, DA12062, DA017186, MH066393, and MH067497.

DISCLOSURE/CONFLICT OF INTEREST

The authors disclose that Greg A Gerhardt is the Director of Operations for Quanteon Limited Liability Company (Nicholasville, KY). Quanteon developed the MEAs and FAST system utilized for these studies. No financial support or compensation was provided on behalf of Quanteon. The authors, therefore, agree that none have financial support, compensation, and personal financial holdings that could be perceived as constituting a potential conflict of interest.

REFERENCES

- Alexander GE, DeLong MR, Strick PL (1986). Parallel organization of functionally segregated circuits linking basal ganglia and cortex. *Annu Rev Neurosci* 9: 357–381.
- Ariano MA, Larson ER, Noblett KL, Sibley DR, Levine MS (1997a). Coexpression of striatal dopamine receptor subtypes and excitatory amino acid subunits. *Synapse* 26: 400–414.
- Ariano MA, Wang J, Noblett KL, Larson ER, Sibley DR (1997b). Cellular distribution of the rat D4 dopamine receptor protein in the CNS using anti-receptor antisera. *Brain Res* 752: 26–34.
- Avale ME, Falzone TL, Gelman DM, Low MJ, Grandy DK, Rubinstein M (2004). The dopamine D4 receptor is essential for hyperactivity and impaired behavioral inhibition in a mouse model of attention deficit/hyperactivity disorder. *Mol Psychiatry* 9: 718–726.
- Bachner-Melman R, Lerer E, Zohar AH, Kremer I, Elizur Y, Nemanov L *et al* (2007). Anorexia nervosa, perfectionism, and

- dopamine D4 receptor (DRD4). *Am J Med Genet B Neuro-psychiatr Genet* **144B**: 748–756.
- Behrens PF, Franz P, Woodman B, Lindenberg KS, Landwehrmeyer GB (2002). Impaired glutamate transport and glutamate-glutamine cycling: downstream effects of the Huntington mutation. *Brain* **125**: 1908–1922.
- Benjamin J, Li L, Patterson C, Greenberg BD, Murphy DL, Hamer DH (1996). Population and familial association between the D4 dopamine receptor gene and measures of Novelty Seeking. *Nat Genet* **12**: 81–84.
- Berger MA, Defagot MC, Villar MJ, Antonelli MC (2001). D4 dopamine and metabotropic glutamate receptors in cerebral cortex and striatum in rat brain. *Neurochem Res* **26**: 345–352.
- Borland LM, Shi G, Yang H, Michael AC (2005). Voltammetric study of extracellular dopamine near microdialysis probes acutely implanted in the striatum of the anesthetized rat. *J Neurosci Methods* **146**: 149–158.
- Burmeister JJ, Gerhardt GA (2001). Self-referencing ceramic-based multisite microelectrodes for the detection and elimination of interferences from the measurement of L-glutamate and other analytes. *Anal Chem* **73**: 1037–1042.
- Burmeister JJ, Moxon K, Gerhardt GA (2000). Ceramic-based multisite microelectrodes for electrochemical recordings. *Anal Chem* **72**: 187–192.
- Burmeister JJ, Pomerleau F, Palmer M, Day BK, Huettl P, Gerhardt GA (2002). Improved ceramic-based multisite microelectrode for rapid measurements of L-glutamate in the CNS. *J Neurosci Methods* **119**: 163–171.
- Carrey N, MacMaster FP, Fogel J, Sparkes S, Waschbusch D, Sullivan S et al (2003). Metabolite changes resulting from treatment in children with ADHD: a 1H-MRS study. *Clin Neuropharmacol* **26**: 218–221.
- Carrey NJ, MacMaster FP, Gaudet L, Schmidt MH (2007). Striatal creatine and glutamate/glutamine in attention-deficit/hyperactivity disorder. *J Child Adolesc Psychopharmacol* **17**: 11–17.
- Cass WA, Gerhardt GA (1995). *In vivo* assessment of dopamine uptake in rat medial prefrontal cortex: comparison with dorsal striatum and nucleus accumbens. *J Neurochem* **65**: 201–207.
- Cass WA, Gerhardt GA, Gillespie K, Curella P, Mayfield RD, Zahniser NR (1993). Reduced clearance of exogenous dopamine in rat nucleus accumbens, but not in dorsal striatum, following cocaine challenge in rats withdrawn from repeated cocaine administration. *J Neurochem* **61**: 273–283.
- Cass WA, Gerhardt GA, Mayfield RD, Curella P, Zahniser NR (1992). Differences in dopamine clearance and diffusion in rat striatum and nucleus accumbens following systemic cocaine administration. *J Neurochem* **59**: 259–266.
- Cooper JR, Bloom FE, Roth RH (2003). *The Biochemical Basis of Neuropharmacology*. Oxford University Press: Oxford.
- Day BK, Pomerleau F, Burmeister JJ, Huettl P, Gerhardt GA (2006). Microelectrode array studies of basal and potassium-evoked release of L-glutamate in the anesthetized rat brain. *J Neurochem* **96**: 1626–1635.
- de Sousa SC, Karwautz A, Wober C, Wagner G, Breen G, Zesch HE et al (2007). A dopamine D4 receptor exon 3 VNTR allele protecting against migraine without aura. *Ann Neurol* **61**: 574–578.
- Defagot MC, Falzone TL, Low MJ, Grandy DK, Rubinstein M, Antonelli MC (2000). Quantitative analysis of the dopamine D4 receptor in the mouse brain. *J Neurosci Res* **59**: 202–208.
- Durston S, Tottenham NT, Thomas KM, Davidson MC, Eigsti IM, Yang Y et al (2003). Differential patterns of striatal activation in young children with and without ADHD. *Biol Psychiatry* **53**: 871–878.
- Ebstein RP, Novick O, Umansky R, Priel B, Osher Y, Blaine D et al (1996). Dopamine D4 receptor (D4DR) exon III polymorphism associated with the human personality trait of Novelty Seeking. *Nat Genet* **12**: 78–80.
- Espey MG, Kustova Y, Sei Y, Basile AS (1998). Extracellular glutamate levels are chronically elevated in the brains of LP-BM5-infected mice: a mechanism of retrovirus-induced encephalopathy. *J Neurochem* **71**: 2079–2087.
- Franklin K, Paxinos G (1997). *The Mouse Brain in Stereotaxic Coordinates*. Academic Press: New York.
- Friedemann MN, Gerhardt GA (1992). Regional effects of aging on dopaminergic function in the Fischer-344 rat. *Neurobiol Aging* **13**: 325–332.
- Gan L, Falzone TL, Zhang K, Rubinstein M, Baldessarini RJ, Tarazi FI (2004). Enhanced expression of dopamine D(1) and glutamate NMDA receptors in dopamine D(4) receptor knockout mice. *J Mol Neurosci* **22**: 167–178.
- Gerhardt G, Rose G, Stromberg I, Conboy G, Olson L, Jonsson G et al (1985). Dopaminergic neurotoxicity of 1-methyl-4-phenyl-1,2,3,6-tetrahydropyridine (MPTP) in the mouse: an *in vivo* electrochemical study. *J Pharmacol Exp Ther* **235**: 259–265.
- Gerhardt GA, Palmer MR (1987). Characterization of the techniques of pressure ejection and microiontophoresis using *in vivo* electrochemistry. *J Neurosci Methods* **22**: 147–159.
- Gerhardt GA, Rose GM, Hoffer BJ (1986). Release of monoamines from striatum of rat and mouse evoked by local application of potassium: evaluation of a new *in vivo* electrochemical technique. *J Neurochem* **46**: 842–850.
- Gerhardt GA, Rose GM, Hoffer BJ (1987). *In vivo* electrochemical demonstration of potassium-evoked monoamine release from rat cerebellum. *Brain Res* **413**: 327–335.
- Grady DL, Chi HC, Ding YC, Smith M, Wang E, Schuck S et al (2003). High prevalence of rare dopamine receptor D4 alleles in children diagnosed with attention-deficit hyperactivity disorder. *Mol Psychiatry* **8**: 536–545.
- Guo G, Tong Y (2006). Age at first sexual intercourse, genes, and social context: evidence from twins and the dopamine D4 receptor gene. *Demography* **43**: 747–769.
- Hai-Bin T, Duan-Zhi Y, Lan Z, Li-Hua W, Chun-Fu Z, Ming-Wei W et al (2005). Dopamine D(4) receptor antagonist 3-(4-[(18)F]fluorobenzyl)-8-methoxy-1,2,3,4-tetrahydrochromeno[3,4-c]pyridin-5-one([(18)F]FMTP): radiosynthesis and *in vivo* characterization in rats. *Appl Radiat Isot* **63**: 333–342.
- Hascup KN, Rutherford EC, Quintero JE, Day BK, Nickell JR, Pomerleau F et al (2006). Second-by-second measures of l-glutamate and other neurotransmitters using microelectrode arrays. In: Michael AC, Borland LM (eds). *Electrochemical Methods for Neuroscience*. CRC Press: Boca Raton, FL. pp 407–450.
- Hebert MA, Gerhardt GA (1999). Age-related changes in the capacity, rate, and modulation of dopamine uptake within the striatum and nucleus accumbens of Fischer 344 rats: an *in vivo* electrochemical study. *J Pharmacol Exp Ther* **288**: 879–887.
- Jaber M, Robinson SW, Missale C, Caron MG (1996). Dopamine receptors and brain function. *Neuropharmacology* **35**: 1503–1519.
- Kennedy RT, Thompson JE, Vickroy TW (2002). *In vivo* monitoring of amino acids by direct sampling of brain extracellular fluid at ultralow flow rates and capillary electrophoresis. *J Neurosci Methods* **114**: 39–49.
- Lichter JB, Barr CL, Kennedy JL, Van Tol HH, Kidd KK, Livak KJ (1993). A hypervariable segment in the human dopamine receptor D4 (DRD4) gene. *Hum Mol Genet* **2**: 767–773.
- Lou HC, Henriksen L, Bruhn P, Borner H, Nielsen JB (1989). Striatal dysfunction in attention deficit and hyperkinetic disorder. *Arch Neurol* **46**: 48–52.
- Luthman J, Friedemann MN, Hoffer BJ, Gerhardt GA (1993). *In vivo* electrochemical measurements of exogenous dopamine clearance in normal and neonatal 6-hydroxydopamine-treated rat striatum. *Exp Neurol* **122**: 273–282.
- MacMaster FP, Carrey N, Sparkes S, Kusumakar V (2003). Proton spectroscopy in medication-free pediatric attention-deficit/hyperactivity disorder. *Biol Psychiatry* **53**: 184–187.

- Maura G, Giardi A, Raiteri M (1988). Release-regulating D-2 dopamine receptors are located on striatal glutamatergic nerve terminals. *J Pharmacol Exp Ther* **247**: 680–684.
- McGeorge AJ, Faull RL (1989). The organization of the projection from the cerebral cortex to the striatum in the rat. *Neuroscience* **29**: 503–537.
- Mrzljak L, Bergson C, Pappy M, Huff R, Levenson R, Goldman-Rakic PS (1996). Localization of dopamine D4 receptors in GABAergic neurons of the primate brain. *Nature* **381**: 245–248.
- Nickell J, Pomerleau F, Allen J, Gerhardt GA (2005). Age-related changes in the dynamics of potassium-evoked L-glutamate release in the striatum of Fischer 344 rats. *J Neural Transm* **112**: 87–96.
- Nickell J, Salvatore MF, Pomerleau F, Apparsundaram S, Gerhardt GA (2007). Reduced plasma membrane surface expression of GLAST mediates decreased glutamate regulation in the aged striatum. *Neurobiol Aging* **28**: 1737–1748.
- Noain D, Avale ME, Wedemeyer C, Calvo D, Peper M, Rubinstein M (2006). Identification of brain neurons expressing the dopamine D4 receptor gene using BAC transgenic mice. *Eur J Neurosci* **24**: 2429–2438.
- Oak JN, Oldenhof J, Van Tol HH (2000). The dopamine D(4) receptor: one decade of research. *Eur J Pharmacol* **405**: 303–327.
- Rivera A, Cuellar B, Giron FJ, Grandy DK, de la Calle A, Moratalla R (2002). Dopamine D4 receptors are heterogeneously distributed in the striosomes/matrix compartments of the striatum. *J Neurochem* **80**: 219–229.
- Rubinstein M, Cepeda C, Hurst RS, Flores-Hernandez J, Ariano MA, Falzone TL *et al* (2001). Dopamine D4 receptor-deficient mice display cortical hyperexcitability. *J Neurosci* **21**: 3756–3763.
- Rubinstein M, Phillips TJ, Bunzow JR, Falzone TL, Dziewczapolski G, Zhang G *et al* (1997). Mice lacking dopamine D4 receptors are supersensitive to ethanol, cocaine, and methamphetamine. *Cell* **90**: 991–1001.
- Russell VA, Sagvolden T, Johansen EB (2005). Animal models of attention-deficit hyperactivity disorder. *Behav Brain Funct* **1**: 9.
- Rutherford EC, Pomerleau F, Huettl P, Stromberg I, Gerhardt GA (2007). Chronic second-by-second measures of L-glutamate in the central nervous system of freely moving rats. *J Neurochem* **102**: 712–722.
- Sagvolden T, Johansen EB, Aase H, Russell VA (2005). A dynamic developmental theory of attention-deficit/hyperactivity disorder (ADHD) predominantly hyperactive/impulsive and combined subtypes. *Behav Brain Sci* **28**: 397–419.
- Seeman P, Guan HC, Van Tol HH (1993). Dopamine D4 receptors elevated in schizophrenia. *Nature* **365**: 441–445.
- Seeman P, Weinschenker D, Quirion R, Srivastava LK, Bhardwaj SK, Grandy DK *et al* (2005). Dopamine supersensitivity correlates with D2High states, implying many paths to psychosis. *Proc Natl Acad Sci USA* **102**: 3513–3518.
- Tarazi FI, Zhang K, Baldessarini RJ (2004). Dopamine D4 receptors: beyond schizophrenia. *J Recept Signal Transduct Res* **24**: 131–147.
- Teicher MH, Anderson CM, Polcari A, Glod CA, Maas LC, Renshaw PF (2000). Functional deficits in basal ganglia of children with attention-deficit/hyperactivity disorder shown with functional magnetic resonance imaging relaxometry. *Nat Med* **6**: 470–473.
- Thomas TC, Kruzich PJ, Joyce BM, Gash CR, Suchland K, Surgener SP *et al* (2007). Dopamine D4 receptor knockout mice exhibit neurochemical changes consistent with decreased dopamine release. *J Neurosci Methods* **166**: 306–314.
- Zhang K, Davids E, Tarazi FI, Baldessarini RJ (2002). Effects of dopamine D4 receptor-selective antagonists on motor hyperactivity in rats with neonatal 6-hydroxydopamine lesions. *Psychopharmacology (Berl)* **161**: 100–106.
- Zhang K, Tarazi FI, Baldessarini RJ (2001). Role of dopamine D(4) receptors in motor hyperactivity induced by neonatal 6-hydroxydopamine lesions in rats. *Neuropsychopharmacology* **25**: 624–632.